Acta Crystallographica Section C
Crystal Structure Communications
ISSN 0108-2701

4-(3,5-Dimethyl-1*H*-pyrazol-4-ylmethyl)-3,5-dimethyl-1*H*-pyrazol-2-ium dihydrogen phosphate: a combined X-ray and DFT study

Dipak K. Hazra,[a] Rajarshi Chatterjee,[b] Mahammad Ali[b] and Monika Mukherjee[a]*

[a]Department of Solid State Physics, Indian Association for the Cultivation of Science, Jadavpur, Kolkata 700 032, India, and [b]Department of Chemistry, Jadavpur University, Kolkata 700 032, India
Correspondence e-mail: sspmm@iacs.res.in

Received 1 February 2010
Accepted 24 February 2010
Online 6 March 2010

The molecular structure of the title salt, $C_{11}H_{17}N_4^+\cdot H_2PO_4^-$, has been determined from single-crystal X-ray analysis and compared with the structure calculated by density functional theory (DFT) at the BLYP level. The crystal packing in the title compound is stabilized primarily by intermolecular N—H···O, O—H···N and O—H···O hydrogen bonds and π–π stacking interactions, and thus a three-dimensional supramolecular honeycomb network consisting of $R_4^2(10)$, $R_4^4(14)$ and $R_4^4(24)$ ring motifs is established. The HOMO–LUMO energy gap (1.338 eV; HOMO is the highest occupied molecular orbital and LUMO is the lowest unoccupied molecular orbital) indicates a high chemical reactivity for the title compound.

Comment

Hybrid organic–inorganic adducts are of current interest due to their intriguing architectures and potential applications in crystal engineering (Ma *et al.*, 2009; Almeida Paz *et al.*, 2004). The intermolecular forces between the different components of these hybrid crystals are provided by hydrogen-bonding or other non-covalent and non-ionic interactions (Almarsson & Zaworotko, 2004). Among the various compounds available for studying phosphoric acid–ligand interactions, amines and *N*-unsubstituted pyrazoles possessing one or more active lone pairs have been frequently used (Turki *et al.*, 2006; Elaoud *et al.*, 2000). The strong N—H···O hydrogen bonds and possible π–π stacking in these hybrid systems facilitate molecular assemblies with one-dimensional chains, two-dimensional layers or three-dimensional frameworks (Turner & Batten, 2008; Oueslati *et al.*, 2006). The recurring structural ensembles in these structures, referred to as synthons (Desiraju, 1995), have been used as building blocks for designing new crystalline materials. Several monophosphate ion–organic ligand hybrid systems also display interesting physical properties, such as ferroelectricity, piezoelectricity and nonlinear optical phenomena (Masse *et al.*, 1993). As part of an ongoing study on the synthesis and structural characterization of new phosphate salts of substituted bis-pyrazole systems, we synthesized the title compound, (I), designed for self-complexation, and the crystal structure was established by single-crystal X-ray analysis along with its electronic structure evaluation using density functional theory (DFT).

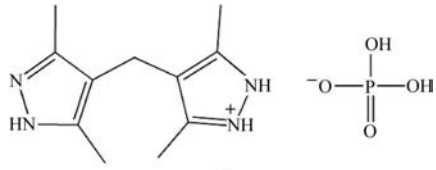

(I)

The asymmetric unit of (I) consists of a 4-(3,5-dimethyl-1*H*-pyrazol-4-ylmethyl)-3,5-dimethyl-1*H*-pyrazol-2-ium (mdmp) cation and a dihydrogen phosphate counter-anion (Fig. 1). The molecular conformation of the mdmp cation can be defined in terms of two torsion angles, *viz.* C5—C6—C7—C10 of −44.3 (5)° and C1—C5—C6—C7 of −57.8 (5)°. The two pyrazole rings (*A* and *B*) are essentially planar, with r.m.s. fits of the atomic positions of 0.001 Å for ring *A* and 0.003 Å for ring *B*. The twist about the methylene bridge in the mdmp cation is reflected by the dihedral angle of 82.2 (2)° between the pyrazole rings; the corresponding value in a crystal of mdmp without any phosphate counter-ion is 81.7 (2)°. The deviation of the *A*/*B* dihedral angle in (I) [82.2 (2)°] from that observed in 4,4′-methylenebispyrazole [90.3 (1)°; Monge *et al.*, 1994], in which both the pyrazole rings are unsubstituted, is probably due to repulsive interactions between the methyl groups and the H atoms of the methylene bridge.

The N—N bond length in pyrazole rings generally varies over a wide range [1.234 (8)–1.385 (4) Å], depending on the substituents at the N atoms (Kettmann & Světlík, 2002).

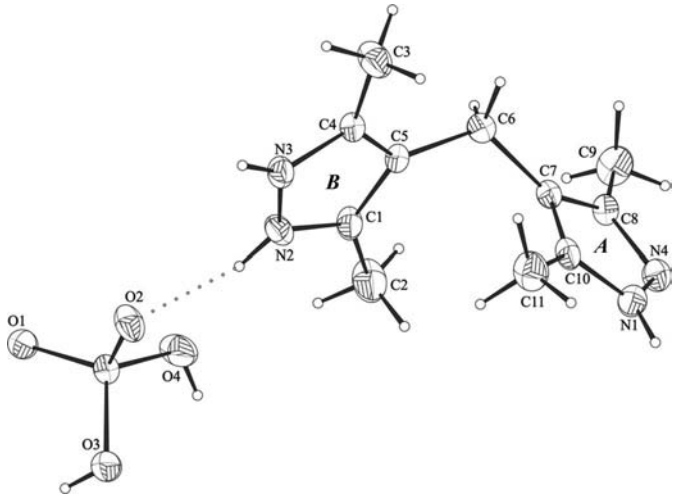

Figure 1
A view of (I), showing the atom-numbering scheme. Displacement ellipsoids are drawn at the 30% probability level and H atoms are shown as small spheres of arbitrary radii. The dotted line indicates an N—H···O hydrogen bond.

  doi:10.1107/S0108270110007134

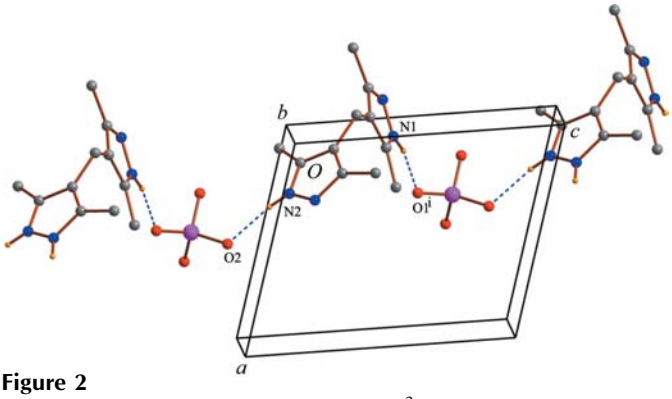

Figure 2
The network of hydrogen bonds forming a $C_2^2(12)$ chain running along the [011] direction. H atoms not participating in this hydrogen-bond chain have been omitted for clarity. [Symmetry code: (i) x, $1 + y$, $1 + z$.]

Accordingly, the adjacent C—N distances range from 1.288 (4) to 1.461 (8) Å. The conjugation within the π-electron system of the pyrazole rings in (I) is reflected in the N—N [1.346 (4)–1.349 (4) Å] and C—N [1.341 (4)–1.350 (4) Å] bond lengths (Table 1), which are intermediate between a single and a double bond and agree with those reported in the literature (Monge *et al.*, 1994; Masse & Tordjman, 1990). The P—O [1.496 (2)–1.523 (2) Å] and P—OH [1.535 (3)–1.565 (2) Å] bond distances in (I) are comparable with the reported values for related phosphates (Oueslati *et al.*, 2006; Turki *et al.*, 2006; Smirani *et al.*, 2004).

As often observed in this kind of system, the two components of (I), *i.e.* the mdmp and $H_2PO_4^-$ ions, are connected through a network of hydrogen bonds and aromatic π–π stacking, in which both pyrazole rings participate (Table 2). It is convenient to consider the substructures generated by different kinds of hydrogen bond acting individually, and then the combination of substructures to build a supramolecular assembly.

Centrosymmetrically related phosphate tetrahedra are connected through pairs of O3—H3*A*···O1($-x + 1$, $-y$, $-z + 1$) hydrogen bonds, which according to graph-set notation (Bernstein *et al.*, 1995) can be described as an $R_2^2(8)$ ring centred at ($\frac{1}{2}$, 0, $\frac{1}{2}$). Intermolecular N1—H1···O1(x, $y + 1$, $z + 1$) and N2—H2···O2 hydrogen bonds link the mdmp cation and phosphate anion into a polymeric $C_2^2(12)$ chain propagating along the [011] direction, as shown in Fig. 2. Similarly, another $C_2^2(12)$ chain running along the [$\bar{1}$10] direction is formed by intermolecular N3—H3···O2($-x + 1$, $-y$, $-z$) and O4—H4···N4($-x$, $-y + 1$, $-z$) hydrogen bonds. The interactions mentioned above generate two types of supramolecular arrangement. In the first, two phosphate anions at (x, y, z) and ($-x + 1$, $-y$, $-z$), together with the pyrazole *B* rings of mdmp cations at ($-x + 1$, $-y$, $-z$) and (x, y, z), give rise to the formation of a cyclic $R_4^2(10)$ synthon having its symmetry centre at ($\frac{1}{2}$, 0, 0) (Fig. 3). The second $R_4^4(14)$ synthon (Fig. 3) is formed by two $H_2PO_4^-$ anions at (x, y, z) and ($-x$, $-y$, $-1 - z$) and two pyrazole *A* rings of cations at ($-x$, $1 - y$, $-z$) and (x, $y - 1$, $z - 1$), with a symmetry centre at (0, 0, $-\frac{1}{2}$). Propagation of the $R_4^2(10)$ and $R_4^4(14)$ rings through lattice translations generates an $R_4^4(24)$ synthon

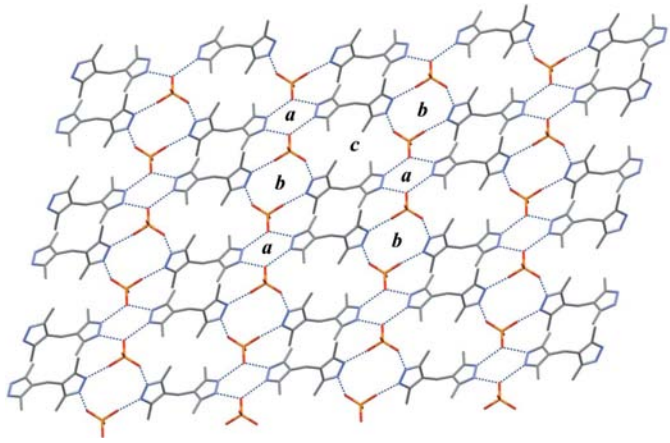

Figure 3
Part of the crystal structure of (I), viewed down [11$\bar{1}$], showing the combination of $R_4^2(10)$ (denoted *a*) and $R_4^4(14)$ (denoted *b*) rings fused alternately, producing $R_4^4(24)$ synthons (denoted *c*), organized in a honeycomb-type three-dimensional supramolecular hydrogen-bonded network. H atoms have been omitted for clarity.

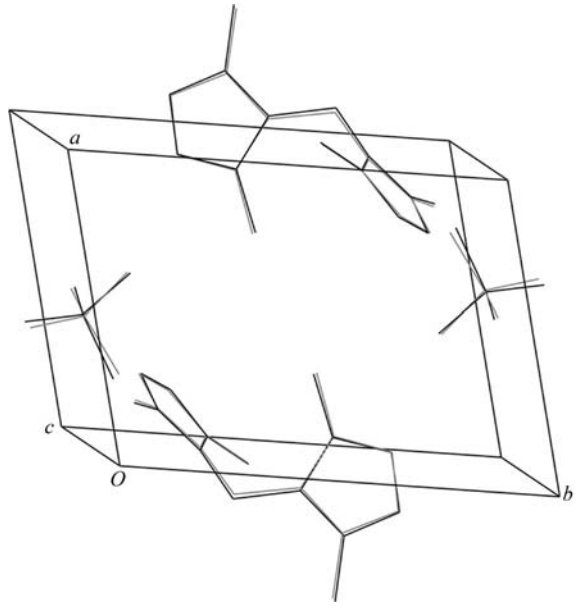

Figure 4
Superposition of the molecules of (I) obtained from the X-ray analysis (lighter-coloured lines) and solid-state DFT calculations (darker-coloured lines).

centred at (0, $\frac{1}{2}$, 0), which in combination with the other ring motifs forms a three-dimensional molecular framework. Viewed down [11$\bar{1}$], the three-dimensional network appears as a honeycomb structure of fused hydrogen-bonded rings (Fig. 3).

The molecular packing in (I) facilitates π–π interactions. The pyrazole *B* rings of centrosymmetrically related mdmp cations form a π–π stacking interaction across the inversion centre at (0, 0, 0); the interplanar spacing and centroid separation are 3.4467 (16) and 3.474 (3) Å, respectively, corresponding to a centroid offset of 0.432 Å.

Solid-state density functional theory (DFT) calculations of (I) have been performed using the *DMOL*^{3} code (Delly, 1996,

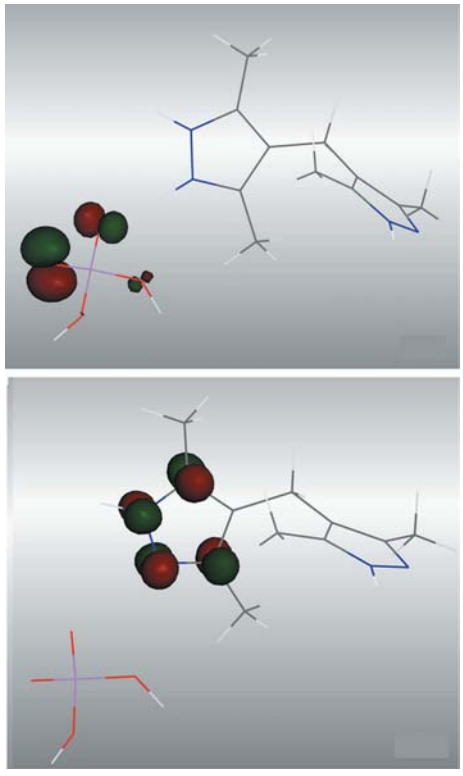

Figure 5
Charge density of the HOMO for (I) (top) and that of the LUMO (bottom), both calculated by DFT.

1998) in the framework of a generalized-gradient approximation (GGA) (Perdew *et al.*, 1996). The starting atomic coordinates were taken from the final X-ray refinement cycle. The geometry of the system was fully optimized using the hybrid exchange-correlation function BLYP (Becke, 1988; Lee *et al.*, 1988) and a double numeric plus polarization (DNP) basis set. The cell parameters were kept fixed during the DFT calculations. No constraints were applied to bond lengths, bond angles or dihedral angles during the calculations, and all atoms were free to optimize.

A superposition of molecular conformations of (I), as established by the X-ray study and quantum mechanical calculations, shows good agreement (Fig. 4); the r.m.s. deviation between the coordinates obtained by geometry optimization and X-ray structure analysis is 0.025 Å. The net charges of atoms and dipoles and the molecular orbital energy of (I) calculated at the BLYP level are listed in Table 3. The O and N atoms in (I) bear negative charges, while atom P1 bears a positive charge. The C atoms of the pyrazole rings bearing methyl substituents (C1, C4, C8 and C10) have positive charges, while the bridging (C6) and methyl C atoms (C2, C3, C9 and C11) have negative charges. The bridgehead C atoms of rings *A* (C7) and *B* (C5) are almost neutral. The orbital energy level analysis for (I) at the BLYP level shows E_{HOMO} (highest occupied molecular orbital) and E_{LUMO} (lowest unoccupied molecular orbital) values of −3.791 and −2.453 eV, respectively. The HOMO–LUMO energy separation has been used as a simple indicator of kinetic stability (Aihara, 1999; Kim *et al.*, 2005). The small HOMO–LUMO gap in (I) (1.338 eV) probably indicates a high chemical reactivity for the title compound. The charge densities for the HOMO and LUMO are shown in Fig. 5.

Experimental

A suspension containing 3,5-dimethylpyrazole (0.192 g, 0.02 mmol) and H_3PO_4 (0.49 g, 5 mmol) in distilled water (30 ml) was stirred thoroughly for 30 min at ambient temperature. The suspension was transferred into a Teflon jacket in a stainless steel pressure vessel and kept in an oven at 433 K for 3 d under autogenous pressure. The solution was then cooled slowly to ambient temperature to yield light-brown crystals of (I) suitable for X-ray diffraction analysis.

Crystal data

$C_{11}H_{17}N_4^+\cdot H_2PO_4^-$
M_r = 302.27
Triclinic, $P\overline{1}$
a = 7.649 (4) Å
b = 10.504 (2) Å
c = 10.538 (2) Å
α = 117.624 (3)°
β = 104.576 (4)°
γ = 94.663 (4)°
V = 706.4 (5) Å^3
Z = 2
Mo $K\alpha$ radiation
μ = 0.21 mm^{-1}
T = 298 K
0.35 × 0.23 × 0.02 mm

Data collection

Bruker APEXII KappaCCD area-detector diffractometer
Absorption correction: multi-scan (*SADABS*; Bruker, 2001)
T_{min} = 0.933, T_{max} = 0.986
4686 measured reflections
2239 independent reflections
1536 reflections with $I > 2\sigma(I)$
R_{int} = 0.036

Refinement

$R[F^2 > 2\sigma(F^2)]$ = 0.052
$wR(F^2)$ = 0.136
S = 1.03
2239 reflections
189 parameters
H-atom parameters constrained
$\Delta\rho_{max}$ = 0.20 e Å^{-3}
$\Delta\rho_{min}$ = −0.38 e Å^{-3}

Table 1
Selected geometric parameters (Å, °).

P1—O1	1.496 (2)	N1—C10	1.350 (4)
P1—O2	1.523 (2)	N2—C1	1.341 (4)
P1—O3	1.565 (2)	N2—N3	1.346 (4)
P1—O4	1.535 (3)	N3—C4	1.344 (4)
N1—N4	1.349 (4)	N4—C8	1.341 (4)
C1—C5—C6—C7	−57.8 (5)	C5—C6—C7—C10	−44.3 (5)

Table 2
Hydrogen-bond geometry (Å, °).

D—H···A	D—H	H···A	D···A	D—H···A
N1—H1···O1^{i}	0.86	1.89	2.726 (4)	164
N2—H2···O2	0.86	1.96	2.789 (4)	161
N3—H3···O2^{ii}	0.86	1.79	2.649 (4)	178
O3—H3*A*···O1^{iii}	0.82	1.83	2.639 (3)	169
O4—H4···N4^{iv}	0.82	1.85	2.571 (4)	146

Symmetry codes: (i) $x, y+1, z+1$; (ii) $-x+1, -y, -z$; (iii) $-x+1, -y, -z-1$; (iv) $-x, -y+1, -z$.

All H atoms were located in difference Fourier maps but were subsequently placed in geometrically optimized positions and treated as riding, with C—H = 0.96–0.97 Å, N—H = 0.86 Å or O—H = 0.82 Å

Table 3
Net charge of atoms and dipoles, and the molecular orbital energies of (I).

Atom	Charge	Atom	Charge
P1	1.435	C10	0.145
N1	−0.152	C7	−0.036
N2	−0.118	C4	0.178
N3	−0.149	C5	−0.006
N4	−0.244	C8	0.101
O1	−0.741	C11	−0.253
O2	−0.821	C3	−0.250
O3	−0.623	C2	−0.263
O4	−0.630	C6	−0.230
C1	0.173	C9	−0.231
Dipole (a.u.)	5.58976		
$E_{binding}$ (eV)	−173.12		
E_{HOMO} (eV)	−3.791	E_{LUMO} (eV)	−2.453

and with $U_{iso}(H) = 1.2U_{eq}(C,N)$ or $1.5U_{eq}(O)$. A common isotropic displacement parameter was refined for the methyl H atoms. The best crystal available was a thin plate (0.35 × 0.23 × 0.02 mm), which diffracted weakly at higher angles, so data collection was terminated at $\theta = 24.2^{\circ}$. Despite this, the title structure was refined using 99% of the possible data, which is considered adequate to give a precise structure.

Data collection: *APEX2* (Bruker, 2007); cell refinement: *APEX2* and *SAINT* (Bruker, 2007); data reduction: *SAINT* and *XPREP* (Bruker, 2007); program(s) used to solve structure: *SHELXS97* (Sheldrick, 2008); program(s) used to refine structure: *SHELXL97* (Sheldrick, 2008); molecular graphics: *ORTEP-3 for Windows* (Farrugia, 1997), *DIAMOND* (Brandenburg, 1999) and *Mercury* (Macrae *et al.*, 2006); software used to prepare material for publication: *PLATON* (Spek, 2009).

The authors thank Professor A. K. Mukherjee, Department of Physics, Jadavpur University, for his interest, help and stimulating discussions. DKH is grateful to the DST-funded National Single-Crystal X-ray Diffraction Facility at the Department of Inorganic Chemistry, IACS, for the data collection.

Supplementary data for this paper are available from the IUCr electronic archives (Reference: SK3363). Services for accessing these data are described at the back of the journal.

References

Aihara, J. (1999). *J. Phys. Chem. A*, **103**, 7487–7495.
Almarsson, O. & Zaworotko, M. J. (2004). *Chem. Commun.* pp. 1889–1896.
Almeida Paz, F. A., Sousa, F. L., Soares-Santos, P. C. R., Cavaleiro, A. M. V., Nogueira, H. I. S., Klinowski, J. & Trindade, T. (2004). *Acta Cryst.* E**60**, m1–m5.
Becke, A. D. (1988). *Phys. Rev. A*, **38**, 3098–3100.
Bernstein, J., Davis, R. E., Shimoni, L. & Chang, N.-L. (1995). *Angew. Chem. Int. Ed. Engl.* **34**, 1555–1573.
Brandenburg, K. (1999). *DIAMOND*. Crystal Impact GbR, Bonn, Germany.
Bruker (2001). *SADABS*. Bruker AXS Inc., Madison, Wisconsin, USA.
Bruker (2007). *APEX2*, *SAINT* and *XPREP*. Bruker AXS Inc., Madison, Wisconsin, USA.
Delly, B. (1996). *J. Phys. Chem.* **100**, 6107–6110.
Delly, B. (1998). *Int. J. Quantum Chem.* **69**, 423–433.
Desiraju, G. R. (1995). *Angew. Chem. Int. Ed. Engl.* **34**, 2311–2327.
Elaoud, Z., Kamoun, S., Mhiri, T., Romain, F. & Burzlaff, H. (2000). *J. Solid State Chem.* **155**, 298–304.
Farrugia, L. J. (1997). *J. Appl. Cryst.* **30**, 565.
Kettmann, V. & Světlík, J. (2002). *Acta Cryst.* C**58**, o423–o424.
Kim, K. H., Han, Y. K. & Jung, J. (2005). *Theor. Chem. Acc.* **113**, 233–237.
Lee, C., Yang, W. & Parr, R. G. (1988). *Phys. Rev. B*, **37**, 785–789.
Ma, L. F., Wang, L. Y., Wang, Y. Y., Du, M. & Wang, J. G. (2009). *CrystEngComm*, **11**, 109–117.
Macrae, C. F., Edgington, P. R., McCabe, P., Pidcock, E., Shields, G. P., Taylor, R., Towler, M. & van de Streek, J. (2006). *J. Appl. Cryst.* **39**, 453–457.
Masse, R., Bagieu-Beucher, M., Pecault, J., Levy, J. P. & Zyss, J. (1993). *Mol. Cryst. Liq. Cryst. Sci. Technol. B Nonlinear Opt.* **5**, 413–423.
Masse, R. & Tordjman, I. (1990). *Acta Cryst.* C**46**, 606–609.
Monge, M. A., Puebla, E. G., Elguero, J., Toiron, C., Meutermans, W. & Sobrados, I. (1994). *Spectrochim. Acta A*, **50**, 727–734.
Oueslati, J., Oueslati, A., Ben Nasr, C. & Lefebvre, F. (2006). *Solid State Sci.* **8**, 1067–1073.
Perdew, J. P., Burke, K. & Ernzerhof, M. (1996). *Phys. Rev. Lett.* **77**, 3865–3868.
Sheldrick, G. M. (2008). *Acta Cryst.* A**64**, 112–122.
Smirani, W., Slimane, A. B. & Rzaigui, M. (2004). *Z. Kristallogr. New Cryst. Struct.* **219**, 189–190.
Spek, A. L. (2009). *Acta Cryst.* D**65**, 148–155.
Turki, I., Elaoud, Z., Mhiri, T., Kamoun, S., Gravereau, P. & Pechev, S. (2006). *J. Chem. Crystallogr.* **36**, 111–116.
Turner, D. R. & Batten, S. R. (2008). *CrystEngComm*, **10**, 170–172.